THE JOURNAL OF COMPARATIVE NEUROLOGY 249: 261-278 (1986)

The Central Projections of Intracellularly Labeled Auditory Nerve Fibers in Cats: An Analysis of Terminal Morphology

E.M. ROUILLER, R. CRONIN-SCHREIBER, D.M. FEKETE, AND D.K. RYUGO
Department of Anatomy and Cellular Biology, Harvard Medical School, Boston, 02115, and Eaton-Peabody Laboratory, Massachusetts Eye and Ear Infirmary, Boston, 02114

ABSTRACT

The axons of physiologically characterized spiral ganglion neurons (type I) were stained throughout their arborizations in the cochlear nucleus by the intracellular injection of horseradish peroxidase (HRP). The tips of the axonal branches were marked by distinct swellings, ranging in size and shape from small boutons to large perisomatic ramifications. Electron microscopic analysis of such swellings revealed ultrastructural features characteristic of primary auditory synapses, consistent with the hypothesis that terminal swellings identifiable in the light microscope represent presynaptic endings. On the basis of light microscopic differences in size, these endings were organized into three categories.

Endings of relatively small size (terminal boutons, free endings, boutons with filopodia, string endings, and small complex endings) composed 94% of all terminal endings. Within this category of small endings, there were predictable variations in relative size and regional distribution that related to the spontaneous discharge rate (SR) of the fiber. The endings of low and medium SR fibers (SR $\leq$ 18 spikes/second) were smaller on average than those of high SR fibers (SR > 18 spikes/second). Furthermore, there were more endings arising from the ascending branch than from the descending branch when comparing fibers of the low and medium SR group with those of the high SR group. There were not, however, obvious morphological features of this ending category that correlated with the characteristic frequency (CF, the pure tone frequency to which the neuron is most sensitive).

A second category contained medium-sized complex endings, most of which formed axosomatic contacts. This category composed 4% of the population and was found in close proximity to the perikarya of globular, octopus, and spherical cells. The endings from low and medium SR fibers were smaller on average than those from high SR fibers. These endings did not vary in their parent branch distribution with respect to fiber SR, nor did they exhibit morphological features that correlated with fiber CF.

The third category contained large complex endings (endbulbs of Held) and composed 2% of the ending population. Within the anteroventral cochlear nucleus, these large, complex endings made axosomatic contact with spherical cells in the anterior division and with globular cells in the posterior division. There were no systematic variations in ending size or branch distribution that correlated with fiber SR. There was, however, a relationship between ending size and fiber CF such that fibers having CFs below 4 kHz gave rise to the largest endbulbs.

Accepted February 11, 1986.

Address reprint requests to Dr. D.K. Ryugo, Department of Anatomy and Cellular Biology, Harvard Medical School, 25 Shattuck Street, Boston, MA 02115.

E.M. Rouiller's present address is Department of Physiology, School of Medicine, Rue du Bugnon 7, 1005 Lausanne, Switzerland.

D.M. Fekete's present address is MRC Cell Biophysics Unit, 26-29 Drury Lane, London WC2B 5RL, England.

A diverse set of morphological features was observed for each ending, and endings sharing similar features could be recognized and grouped across separate cat brains. It is noteworthy that endings that differed on the basis of shape also differed with respect to size and distribution in the nucleus. The correspondence of morphological and physiological characteristics within but not across ending categories provides evidence that the proposed organization has functional significance.

Key words: cochlear nucleus, endbulbs, hearing, horseradish peroxidase, primary afferents, spontaneous activity, terminal boutons

In the cat cochlear nucleus, the temporal pattern of incoming auditory nerve discharges is either preserved or modified, and the resulting output signals are distributed to various regions of the brain. This coded representation of acoustic stimuli has been described in terms of the discharge properties of single neurons to simple stimuli (e.g., Kiang, '75). The transformations of particular discharge patterns occur in predictable locations in the cochlear nucleus (e.g., Pfeiffer, '66; Godfrey et al., '75a,b; Bourk, '76), and in many instances, are correlated with particular kinds of structures (Osen, '69; Brawer et al., '74). Although the evidence is indirect, it has been postulated that the signal transformations that occur between auditory nerve fibers and cochlear nucleus neurons are due, at least in part, to specific properties of connectivity between presynaptic endings and postsynaptic neurons (Kiang, '75; Tsuchitani, '78; Cant and Morest, '84). For example, it is hypothesized that the large axosomatic endbulbs of Held are responsible for faithfully initiating postsynaptic discharges with presynaptic activity. This one-for-one transmission preserves the temporal pattern of discharges from one neuron to the next. In contrast, small bouton endings are expected to have much weaker postsynaptic influences, and the resulting increase in transmission failures would tend to transform the signal patterns. In this context, the contribution of presynaptic endings to this coding process is hypothesized to be influenced by certain features of terminal morphology (e.g., size, shape, proximity to postsynaptic spike generator, etc.).

Most descriptions of the terminal morphology of auditory nerve fibers have been derived from Golgi preparations of neonatal or juvenile animals (Held, 1893; Vincenzi, '01; Ramón y Cajal, '09; Feldman and Harrison, '69; Lorente de Nó, '81; Brawer and Morest, '75), and these observations have been used to interpret physiological data regarding mechanisms of stimulus coding in adult animals (e.g., Tsuchitani, '78). There is accumulating evidence, however, that significant age-related changes occur in both the morphology and functional properties of spiral ganglion neurons (Pujol et al., '78, '79; Romand et al., '76, '80; Ryugo and Fekete, '82; Kettner et al., '84; Romand, '84). Thus, it would appear that Golgi descriptions of primary endings in kittens are not accurate for adult cats from which most electrophysiological results have been obtained.

The present report provides a morphological analysis of axon terminals of type I spiral ganglion cells in mature cats. Current methods for marking individual neurons after studying their physiological properties have allowed us to establish direct correspondences between electrophysiologically defined unit types in the auditory nerve and morphological features of their terminal endings in the cochlear nucleus. The endings of these labeled axons were analyzed in order to define structural characteristics that correlate with the specific physiological properties of CF and SR.

MATERIALS AND METHODS

A total of 15 cats, each weighing between 1.75 and 3.4 kg and free of middle ear infections, were used in this study. The anesthetic and surgical preparation, the means of presenting acoustic stimuli, and the techniques for recording and processing single unit activity have been previously described (Kiang et al., '65; Liberman, '78). Specific details for intracellular recording and injecting of individual auditory nerve fibers, procedures for histological processing, and criteria for recovering labeled fibers from tissue sections have also been described (Liberman, '82a,b; Fekete et al., '84).

For each unit, intra-axonal penetration was indicated by a stable negative resting potential; a threshold tuning curve (fully described by Liberman, '78) and a 15- or 30-second sample of spontaneous activity (SR, spikes per second) were obtained before and after the injection of horseradish peroxidase (HRP). The tuning curve was used to determine a unit's CF. SR was defined as activity in the absence of sound controlled by the experimenter. Units were assigned to SR groups by using the criteria of Liberman ('78): low SR = less than 0.5 spikes per second (s/s); medium SR = 0.5–18 s/s; high SR = greater than 18 s/s. The maintenance of a continuous negative resting potential and the similarity of response properties (e.g., spike waveform, SR, and CF) collected before and after the HRP injection provided evidence that the injected fiber corresponded to the physiologically characterized unit. Only one to three units were injected per auditory nerve, and fiber recovery was based on a correspondence of the histological location of the fiber's injection site to the calculated position of the electrode tip at the time of injection.

This report is restricted to a description of the presynaptic endings from type I spiral ganglion neurons that were darkly stained throughout their arborizations and that were recovered with a high degree of confidence. Terminal endings (n=2,060) were drawn by use of a light microscope and drawing tube (total magnification = ×1,250). Once drawn, endings were coded according to their parent branch of origin. The "root" branch was defined as ascending into the cochlear nucleus and bifurcating. This characteristic bifurcation gave rise to an "ascending branch" that was directed anteriorly and a "descending branch" that was directed posteriorly. At a gross level, the separate parent branches were differentially related to different regions of the cochlear nucleus. The ascending branch (AB) and root branch (RB) contributed endings primarily to the anteroventral cochlear nucleus (AVCN), whereas the descending branch (DB) contributed mostly to the posteroventral cochlear nu-

cleus (PVCN) and the dorsal cochlear nucleus (DCN). Endings were then categorized according to the number of component lobes (explained more fully in the Results section) and analyzed with respect to the additional morphological characteristics of silhouette area and postsynaptic target. Ending area was determined by retracing each drawing with a computerized planimeter. Low and medium SR fibers have been grouped together for purposes of comparison to high SR fibers because they tend to share a number of electrophysiological (Liberman, '78; Evans and Palmer, '80; Costalupes, '85) and morphological features (Liberman, '82a; Fekete et al., '84). Within a category, endings were analyzed according to fiber SR group (high SR vs. low-medium SR) and parent branch of origin (AB, DB, RB). For the present time, we have not emphasized RB data because of the relatively small sample of root branch endings. Means, standard errors of the mean, and Student's P values (two-tailed test) are provided where appropriate.

The cytoarchitectonic subdivisions and cell types of the cochlear nucleus used in this paper represent a hybrid of criteria and nomenclature (Osen, '69; Brawer et al., '74; Cant and Morest, '79a; Tolbert and Morest, '82a). In the AVCN, we have defined a superior-frontal region that includes mostly "spherical" cells, recognized by a perinuclear cap of Nissl substance, and "clawlike" endings defined as endbulbs in protargol-stained material. This region coincides with a relatively myelin-sparse zone revealed in hemotoxylin-stained material, and roughly corresponds to the anterior part (AA) and posterodorsal part (APD) of the anterior division of the AVCN (AVCNa). The relative density of spherical cells is gradually reduced in more posterior regions of the AVCNa. This transitional zone forms what is called the posterior part (AP) of the AVCNa.

The posterior division of the AVCN (AVCNp) is characterized by the presence of globular and multipolar cells, and is divided into dorsal (PD) and ventral (PV) parts. The PD displays a more heterogeneous composition of cell types with the occasional appearance of giant cells. In contrast, the PV has a relatively lower density of neurons; it represents the region of the entering auditory nerve, distinguished by the bifurcations of the fibers and the prominent fascicles of ascending branches (AB). Together, the two regions correspond to Osen's ('69) globular cell area.

The PVCN is divided into two major regions (Osen, '69). A central region can be identified by the dominating presence of octopus cells. The remainder of the PVCN surrounds this central region and contains primarily multipolar cells of various sizes and shapes and scattered globular cells. This flanking multipolar cell region contains other small subdivisions (Brawer et al., '74) but they could not always be identified in the present experimental material.

The DCN is separated from the ventral cochlear nucleus by islets of granule cells. This border is distinct and was used in determining whether individual auditory nerve fibers innervated the DCN. The DCN itself is a cortical structure having well-defined layers (e.g., Mugnaini et al., '80). The resulting subdivisional scheme demarcates regions that have been presented previously (see Fig. 2: Fekete et al., '84).

RESULTS

The present results are based on an analysis of 27 fibers with CFs of 0.3–36 kHz and whose SR ranged from near zero to 88 s/s. It is already known that our intracellular technique labels only the type I spiral ganglion neurons whose peripheral processes contact exclusively inner hair cells (Liberman and Oliver, '84) and whose central processes ramify in the cochlear nucleus (Fekete et al., '84). The terminal branches of labeled fibers were typically characterized by distinct swellings at their tips. A selected number (n=20) of identified swellings from different regions of the cochlear nucleus was isolated in smaller Epon blocks, thin-sectioned, and examined with the electron microscope (e.g., Fig. 1). All labeled endings exhibited the characteristic ultrastructural features of primary auditory terminals (e.g., Lenn and Reese, '66; Ibata and Pappas, '76; Cant and Morest, '79b; Ryugo and Fekete, '82; Tolbert and Morest, '82b). In representative sections, endings contained mitochondria and numerous clear, round vesicles approximately 50 nm in diameter. The vesicles accumulated on the presynaptic side of the synapse, in close proximity to a thinning of the intercellular space. A band of dense, fuzzy material characteristically lay within the thinned space. Membrane-associated densities in the postsynaptic cytoplasm gave the synapse an asymmetrical appearance. These preliminary observations are consistent with the hypothesis that the terminal swellings of axon collaterals identifiable in the light microscope truly represent presynaptic endings.

The endings exhibit a wide variety in sizes and shapes. Most appear as single, discrete swellings whereas others are larger, multilobed structures. Certain morphological differences and similarities among individual endings can be discerned, and on the basis of certain shared features, the following separate categories are proposed.

Ending categories

Simple endings. Small, punctate swellings represented 71.1% of all axonal endings. Nearly all of these had smooth and continuously convex surface contours and were called "terminal boutons" (Fig. 2, arrows). They were distributed predominantly in the neuropil although they were occasionally found in the vicinity of cell bodies. The distribution of these endings with respect to ascending vs. descending branch varied with SR (Fig. 3A). High SR fibers had relatively more terminal boutons arising from the DB (53.9%) than from the AB (41.3%). Low and medium SR fibers, however, had more terminal boutons arising from the AB (51.6%) than from the DB (41.4%). In addition, there were size differences when comparing the terminal boutons of different SR groups (Fig. 3B). The average size from high SR fibers ($4.8 \pm 0.14\ \mu m^2$) was greater (Student's t-test, $p<.001$) than that for low and medium SR fibers ($3.1 \pm 0.10\ \mu m^2$).

The "terminal bouton with filopodium" was one form of ending that was rarely observed (on average, less than two per fiber). This type of ending was characterized by a simple bouton from which emanated a thin filament, less than 0.2 μm in diameter and shorter than 10 μm in length (Fig. 2, arrowheads). Only the swelling (not the filopodium) was measured for size analysis. As with terminal boutons, the average size of these endings from high SR fibers ($6.0 \pm 1.15\ \mu m^2$) was greater than that for low and medium SR fibers ($4.4 \pm 0.84\ \mu m^2$).

The other type of infrequent ending occurred when a collateral terminated abruptly without a visible swelling (Fig. 2, open star). These blunt endings were referred to as "free terminals." Because free terminals ended abruptly rather than fading progressively, it seemed unlikely that

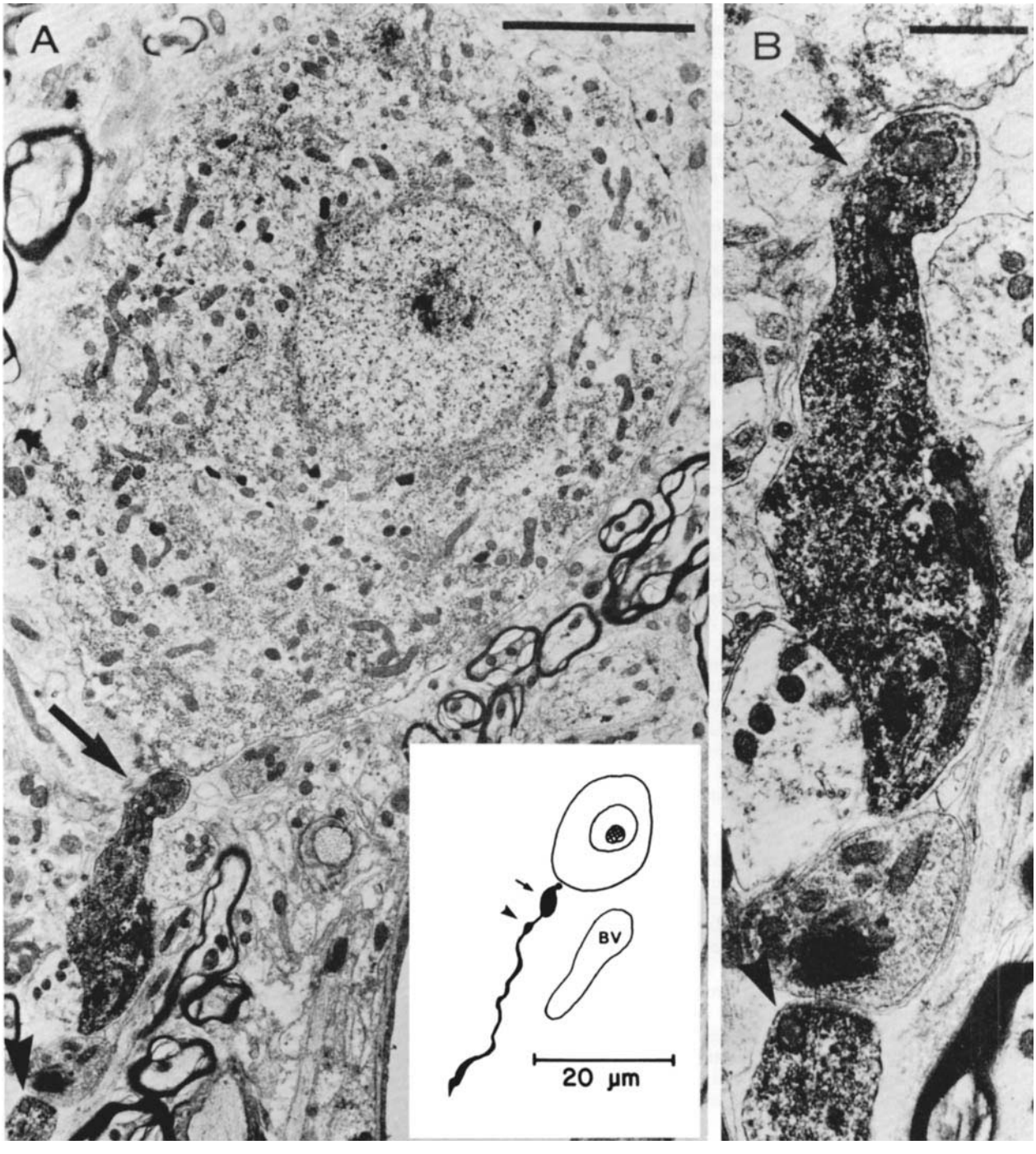

Fig. 1. A. HRP-labeled terminal (arrow) and *en passant* swelling (arrowhead) approaching the cell body of a neuron in the small cell zone of the rostral anteroventral cochlear nucleus (AVCN). Scale bar equals 5 µm. Inset: drawing tube reconstruction of these same terminals. The blood vessel (BV) is also visible at the edge of the inset. B. At higher magnification, the labeled terminal is shown to contain numerous large round vesicles and several mitochondria. This terminal eventually makes a synapse on the cell body, at the base of the dendritic stalk that lies just below. The *en passant* swelling (arrowhead here and in A) has ultrastructural characteristics similar to those of the terminal ending. This swelling appeared to form a synapse on the dendritic shaft, but we could not be certain due to the tangential relationship of the sections to the intercellular space. Scale bar equals 1 micrometer

they represented an artifact due to incomplete staining. Since boundaries between collaterals and these endings were not apparent, their size could not be measured. To date, we have not investigated whether free terminals form synaptic contacts.

String endings. A second general class of ending was represented by the "string" category, composing 11.8% of all endings. String endings were formed by a simple terminal bouton in close proximity to one or more *en passant* swellings (Fig. 4, open arrows). By definition, the compo-

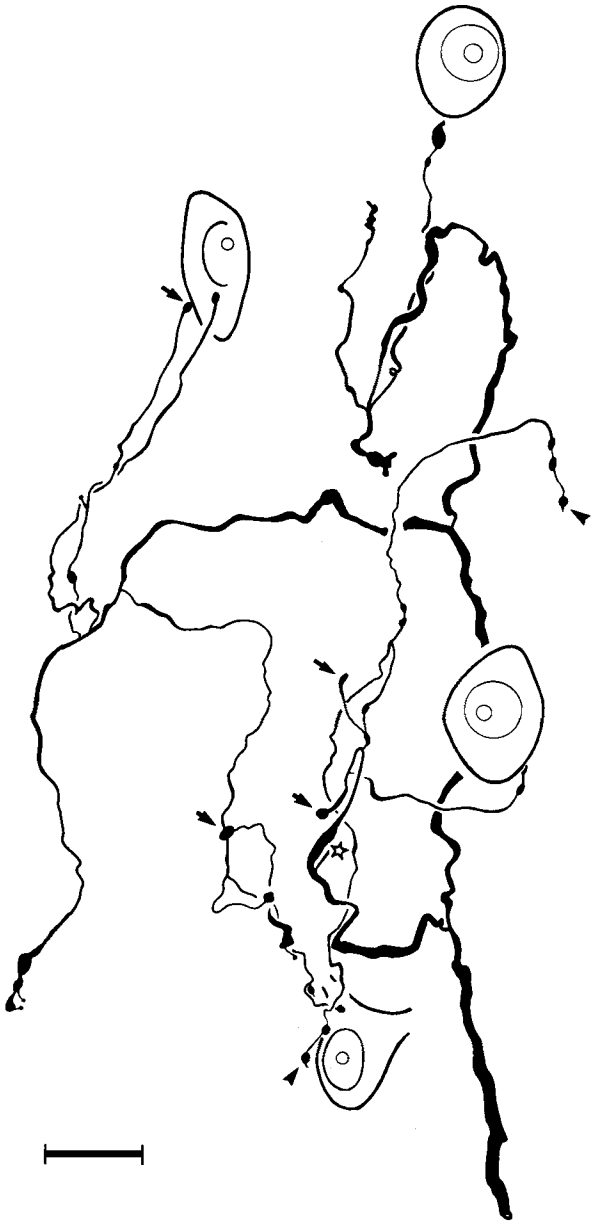

Fig. 2. Drawing tube reconstruction of terminal arborization. This ramification is located within the peripheral cap of small cells in the rostral extreme of the AVCN, just beneath the layer of granule cells. The collateral enters the field from the lower right, ramifies locally, and contacts several cell bodies or terminates in the neuropil. Selected examples of simple endings are indicated: terminal boutons (arrows), free endings, (star), and boutons with filopodia (arrowheads). The cell and terminal branch in the top right of this figure correspond to those shown in Figure 1. Scale bar equals 20 μm.

nents of a string form an array of swellings linked together by thin fiber segments the lengths of which did not exceed the maximal diameter of adjacent swellings. If the length of the distal connecting process exceeded the diameter of the proximal swelling, successive proximal swellings were called *en passant* swellings. Since the components of a string occupied a relatively localized region, they presumably shared the same postsynaptic element (i.e., dendritic shaft).

String endings arose from collaterals of all parent branches and were found throughout the cochlear nucleus (Fig. 5A). High SR fibers have relatively more string endings arising from the DB (59.8%) than from the AB (38.3%). Low and medium SR fibers have relatively more arising from the AB (61%) than from the DB (30%). The size of string endings was on average larger (Student's t-test, $P < .01$) for high SR fibers (10.4 $\pm$ 0.59 μm^2) than for low and medium SR fibers (8.2 $\pm$ 0.47 μm^2). Most (approximately 75%) have only two swellings, but one had a total of eight. The number of swellings did not vary as a function of fiber CF or SR.

Complex endings. A "complex ending" was represented by a relatively large terminal swelling with distinct irregularities (convexities and concavities) along its surface (Fig. 6). Complex endings composed 17.1% of all endings and appeared as a conglomerate of discrete swellings, some of which were fused together; others were interconnected by thin, short processes. These morphologically heterogeneous endings were then separated according to the number of component parts (estimated by counting the varicosities and lobes, where each represented a single component; counting stopped at 50). The criteria (number of components) for group assignment (small, medium, and large) were operationally chosen with the following objectives in mind: (1) to assure that every fiber gave rise to a terminal endbulb (large complex ending); (2) so that small complex endings were roughly similar in size to that of string endings; and (3) to maximize SR-related size differences (*P* values) between the categories (determined by analyzing group differences while varying group composition on the basis of the number of components). These subcategories of complex endings were also distinguishable by their distribution with respect to parent branch of origin (Fig. 7). That is, small and comparatively simple complex endings arose from all parent branches; endings of moderate size and complexity arose primarily from the AB and RB; the largest and most complicated endings arose from the AB.

Small complex endings. These endings were defined as having four or fewer components (Fig. 6a). They represented 11.2% of the total ending population and 65.5% of the complex ending population. Their relative distribution appeared to be related to fiber SR (Fig. 8A). High SR fibers have relatively more small complex endings arising from the DB (53.6%) than from the AB (36.1%). Low and medium SR fibers have more small complex endings arising from the AB (59.4%) than from the DB (36.1%).

There was a wide range in size (0.77–52.4 μm^2) within the population of small complex endings. The largest endings tended to arise from fibers of high SR, whereas the smallest endings tended to arise from fibers of low and medium SR (Fig. 8B). The mean area of those endings arising from high SR fibers (14.1 $\pm$ 0.91 μm^2) was greater (Student's t-test, $P < .01$) than those arising from low and medium SR fibers (10.6 $\pm$ 0.65 μm^2).

Medium complex endings. The endings having 5–13 components (Fig. 6b) composed 3.7% of the total ending population and 21.6% of the complex ending population. These endings typically made axosomatic contact with postsynaptic neurons and probably correspond to the "modified endbulbs" of Harrison and Irving ('66). Modified endbulbs arose throughout the nucleus from thin to moderate-sized axon collaterals (less than 1.5 μm in diameter measured within 10 μm of the swelling). These endings were most abundant in the region of the auditory nerve

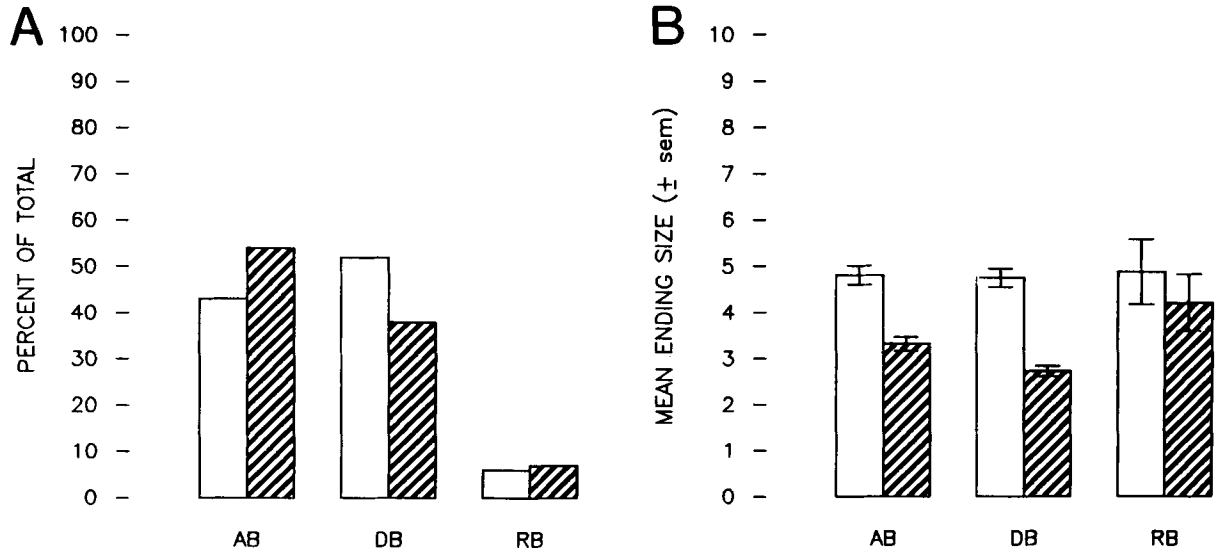

Fig. 3. A. Bar graph illustrating relative branch distribution for all simple endings (terminal boutons, free endings, boutons with filopodia) from fibers of high spontaneous discharge rate (SR) (n=603, open bars) and low and medium SR (n=862, striped bars). B. Bar graph illustrating that simple endings from low and medium SR fibers (striped bars) are generally smaller than those from high SR fibers (open bars) when analyzed according to parent branch of origin: ascending branch (AB) $p < .001$; descending branch (DB), $P < .001$; root branch (RB), P=nonsignificant (n.s.).

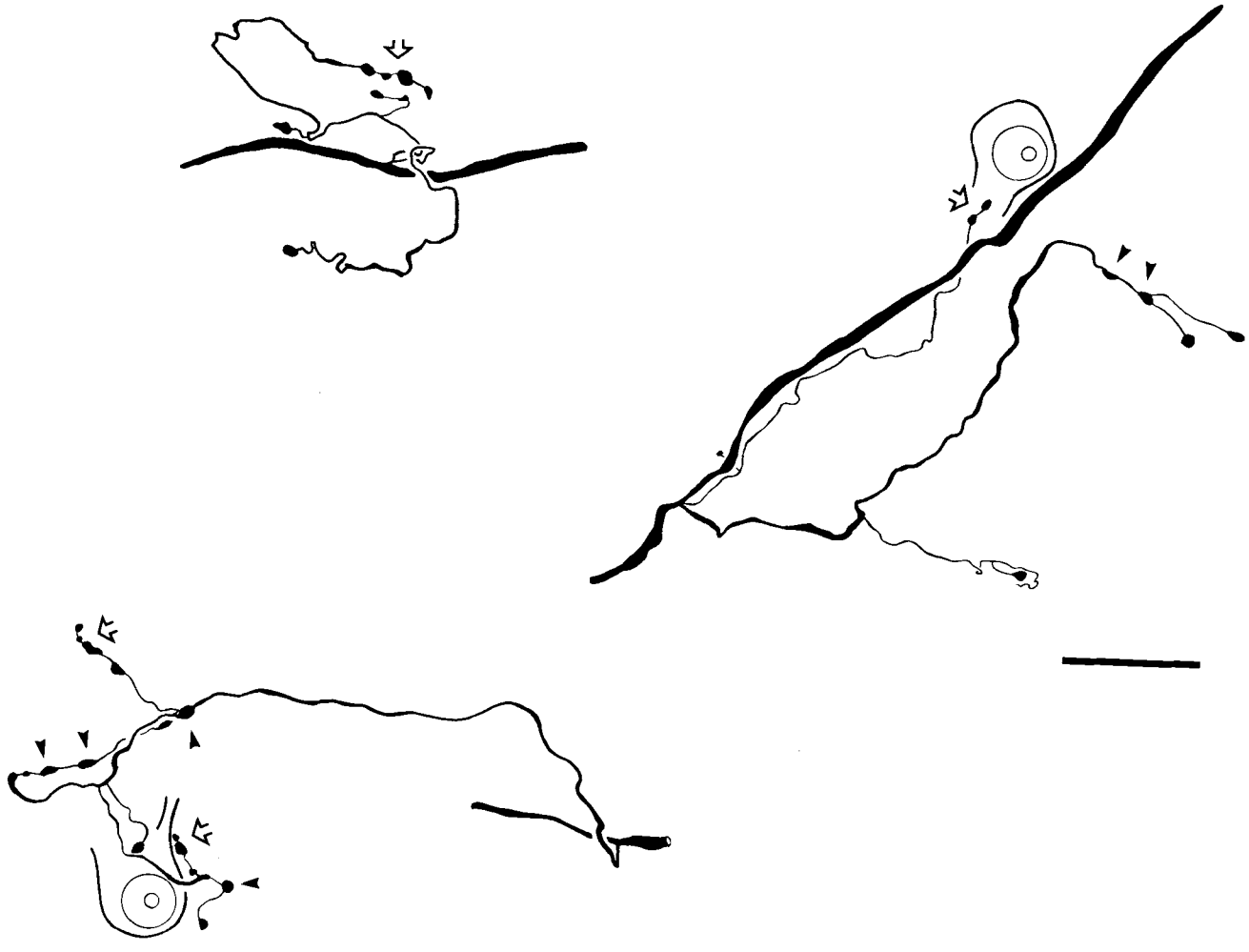

Fig. 4. Drawing tube reconstruction of collateral arborizations that illustrate string endings (open arrows) and *en passant* swellings (arrowheads). These endings have been observed to arise from all parent branches of an individual fiber, and are found throughout the cochlear nucleus. Scale bar equals 20 μm.

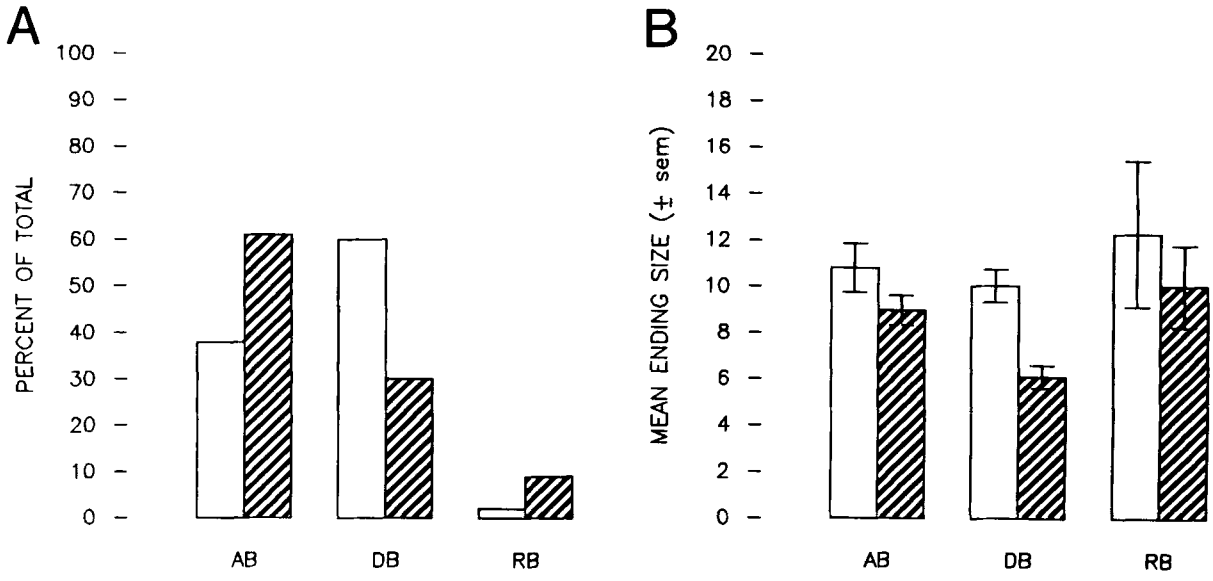

Fig. 5. A. Bar graph illustrating relative branch distribution for all string endings from fibers of high SR (n=107, open bars) and low and medium SR (n=136, striped bars). B. Bar graph illustrating that string endings from low and medium SR fibers (striped bars) can be significantly smaller than those from high SR fibers (open bars) when analyzed according to parent branch of origin: AB, P=n.s.; DB, $P< .001$, RB, P=n.s.

root (AVCNp) where they made axosomatic contacts with globular cells. In several instances, modified endbulbs arose from separate parent branches and converged around the same neuron (Fig. 9). In the AVCNa, modified endbulbs were observed to contact spherical cells.

It has been known for some time that large endings characterize the ascending branch of auditory nerve fibers (e.g., Ramón y Cajal, '09). Less has been reported about relatively large endings or modified endbulbs arising from the descending branch, particularly away from the region of the auditory nerve root. Only a few fibers (five of 27 DBs) gave rise to relatively large endings in the PVCN. Modified endbulbs made axosomatic contact with globular cells (n=4) in the multipolar cell region and with octopus cells (n=5) in the central region (Fig. 10). In the central region, the thicker, relatively unbranched collaterals that gave rise to modified endbulbs were distinctly different from the usual long "streaming" collaterals that branched and terminated in the neuropil as small endings.

There was one example of a medium-to-large ending in the DCN (Fig. 11). This particular "spray" of endings terminated primarily in the neuropil of layer II, but also contacted the perikaryon of a pyramidal cell via a terminal bouton and *en passant* swelling. The presence of these few large endings from the DB was not obviously correlated with CF or SR.

The distribution of modified endbulbs in the cochlear nucleus did not change as a function of fiber SR. Approximately 60% of the modified endbulbs arose from the AB whereas 27% arose from the DB; the remainder arose from the RB (Fig. 12A). Modified endbulbs ranged in size from 12.9 to 125 μm^2, and on average, exhibited a size difference when comparing endings of different SR groups (Fig. 12B). The area of modified endbulbs from high SR fibers (44.0 ± 3.58 μm^2) was on average larger (Student's t-test, $P< .01$) than those of low and medium SR fibers (27.5 ± 2.66 μm^2).

Large complex endings. The largest and most intricate endings corresponded to what have typically been called endbulbs of Held (Fig. 6c). These endings represented 2.2% of the total ending population and 12.9% of the complex ending population. "True" endbulbs were operationally distinguished from other complex endings by (1) their composition of 14 or more elements (varicosities or distinct lobes) and (2) the relatively large diameter of their parent axon (greater than 1.5 micrometers within 10 μm of the terminal swelling). Endbulbs (as defined here) arose either from the ABs (85%) or RBs (15%), and this distribution did not change in any systematic way as a function of fiber SR (Fig. 13A).

The ascending branch of each auditory nerve fiber was marked by the presence of a large axosomatic ending, called the terminal endbulb (Ramón y Cajal, '09; Fekete et al., '84). All other large endings (which arose from primary collaterals of parent branches) were called collateral endbulbs. Each fiber exhibited a terminal endbulb located in the AVCNa. The majority of terminal endbulbs (n=21) were located in the anterior half (AA and APD) of the AVCNa. The remaining endbulbs (n=6) were located in the posterior half (AP and the AA/AP border) of the AVCNa. Terminal endbulbs made axosomatic contact with perikarya having cytological features of spherical (bushy) cells. Collateral endbulbs in AVCNa also terminated on spherical cells, whereas those in AVCNp terminated on globular cells (criteria of Osen, '69; Tolbert and Morest, '82a,b).

The size of terminal endbulbs has been compared to that of collateral endbulbs (Fig. 14A). On average, terminal endbulbs were larger (248.8 ± 22.31 μm^2) than collateral endbulbs (167 ± 24.43 μm^2), although several of the collateral endbulbs contacting globular cells were actually larger than some of the endbulbs (collateral or terminal) contacting spherical cells. Endbulb size was also analyzed with respect to cochlear nucleus subdivisions (Table 1) and according to primary collateral sequence along individual ABs for five randomly selected fibers. Although there was not an absolute relationship between endbulb size and

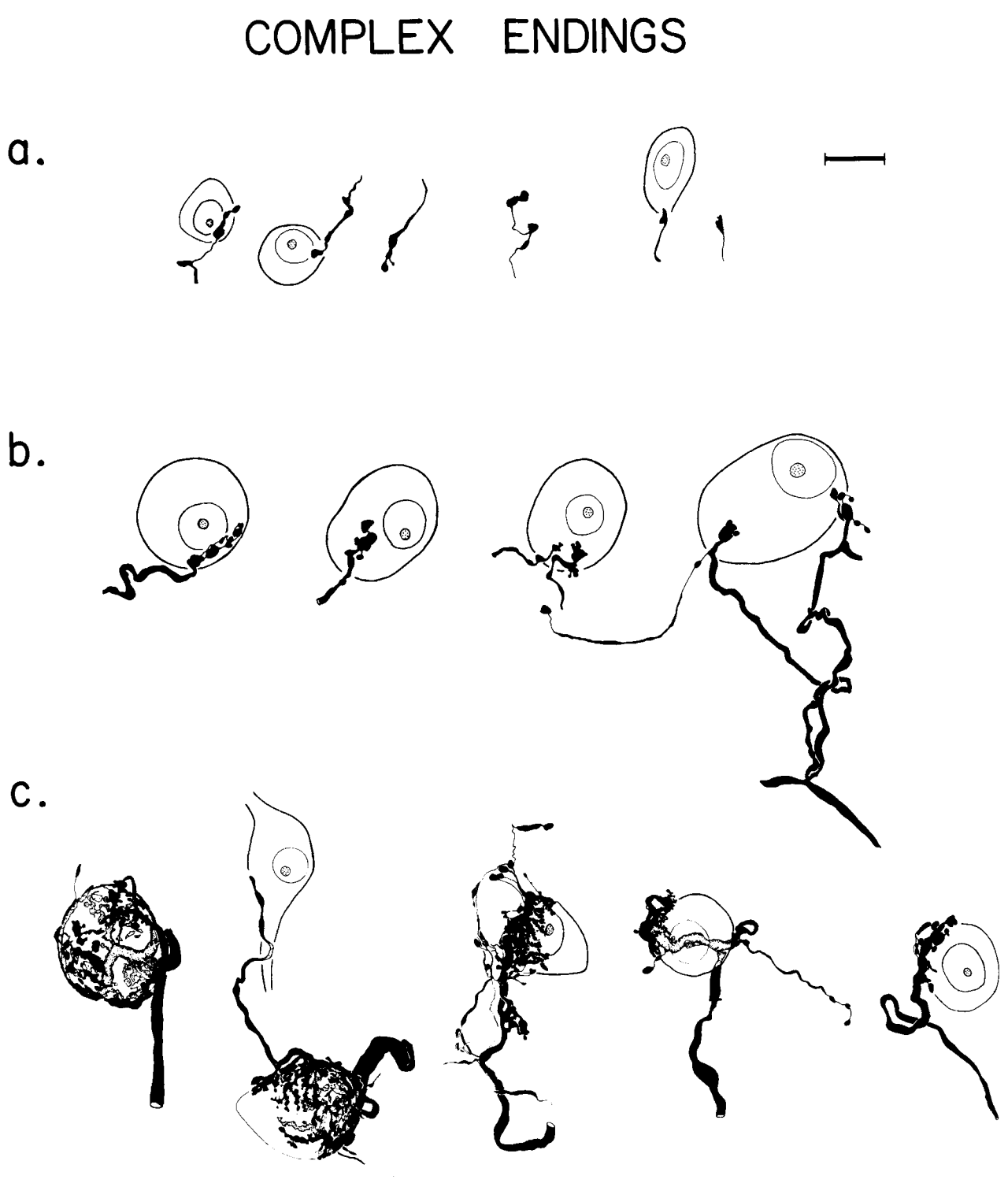

Fig. 6. Drawing tube reconstructions of complex endings and (where visible) postsynaptic neurons. a. Small complex endings arise from thin collaterals. Some terminate in the vicinity of relatively small cell bodies; others terminate in the neuropil. b. Medium-sized complex endings are represented primarily by modified endbulbs. Modified endbulbs usually make axosomatic contact with globular cells (three cells on the left side of the row), although they will also contact spherical cells and occasionally octopus cells (cell on far right of row). c. Large complex endings are best known as endbulbs of Held. The terminal endbulbs illustrated here contact spherical cells in the anterior part (AA) and posterodorsal part (APD) of the AVCNa. Thin filopodia can arise from the endbulb and terminate nearby. The relative size of the endbulbs corresponds to the size of the postsynaptic spherical cell. Scale bar equals 20 μm.

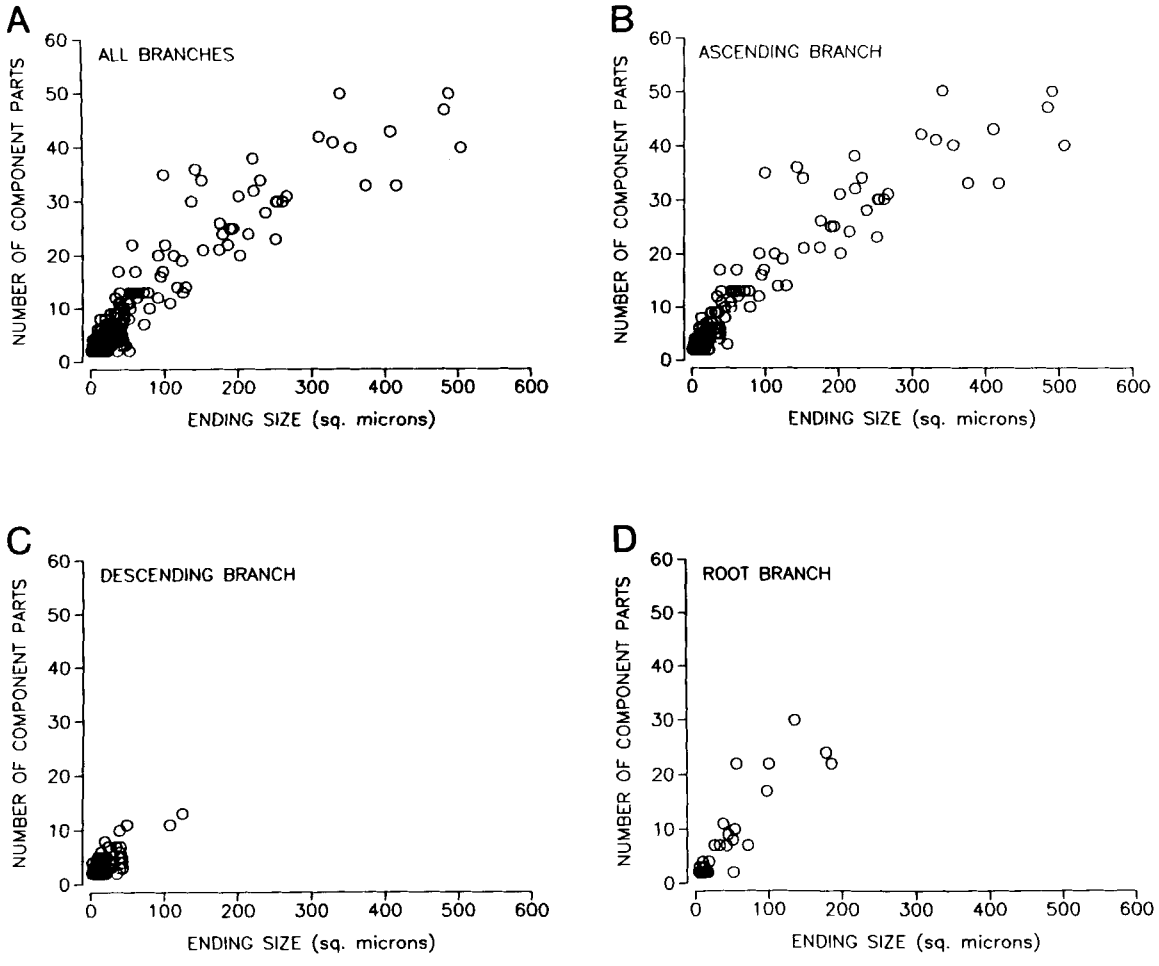

Fig. 7. Representation of complex endings with respect to their parent branch of origin. Ending size is compared to the number of component parts. Small complex endings (< 80 μm^2) arise from all branches. The medium-sized complex endings arise primarily from the AB and RB. The large complex endings arise primarily from the AB.

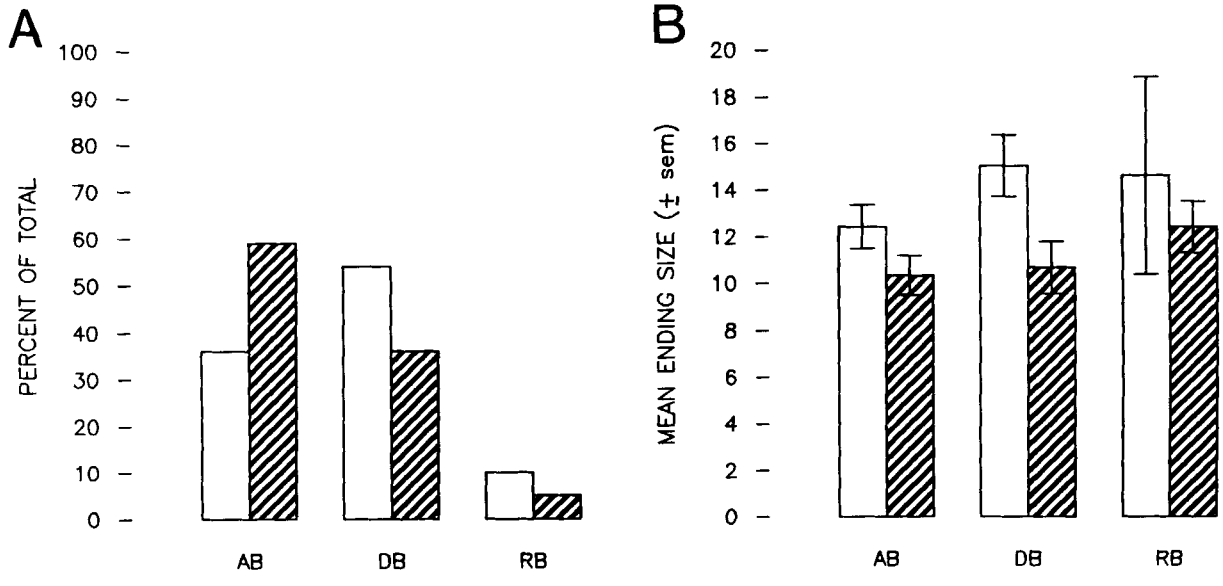

Fig. 8. A. Bar graph illustrating relative branch distribution for all small complex endings from fibers of high SR (n=97, open bars) and low and medium SR (n=133, striped bars). B. Bar graph illustrating that simple endings from low and medium SR fibers (striped bars) are not significantly smaller than those from high SR fibers (open bars) when analyzed according to parent branch of origin: AB, P=n.s.; DB, $P < .02$; RB, P=n.s.

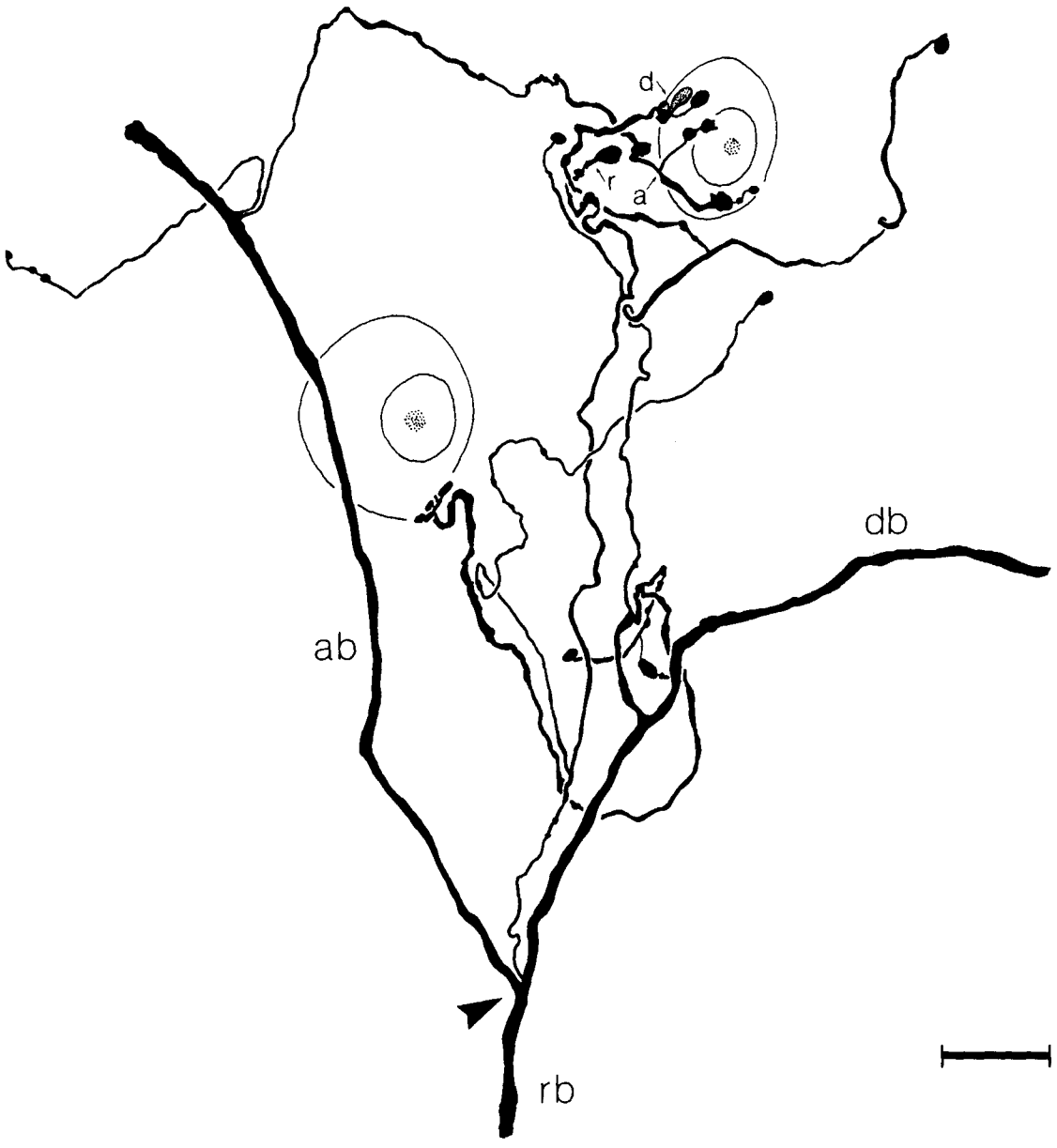

Fig. 9. Drawing tube reconstruction of collateral ramifications in the region (PV) of the bifurcation (arrowhead). Collaterals from each of the parent branches (ab, ascending branch; db, descending branch; rb, root branch) give rise to terminals (respectively, "a", "d", and "r") that converge to within 20 μm of one another. Two collaterals appear to terminate on a small globular cell. The cluster of boutons (r) from the third collateral may terminate on a process of this globular cell, given the close proximity. Scale bar equals 20 μm.

location (whether along an individual fiber or for the population of endbulbs within a subdivision), the data revealed general variations in endbulb size with respect to regional position within the nucleus (such that those in AVCNa < PD < PV).

In addition to the effect CF has on relative position of the endbulb, there were CF-related differences in endbulb size (Fig. 14). The largest endbulbs (terminal as well as collateral) were found on fibers having CFs below 4 kHz; smaller endbulbs (range 80–300 μm^2 but clearly larger than modified endbulbs) were found on fibers spanning the entire CF range. If these largest endbulbs (n=10) were analyzed separately (as if they represent a special subpopulation rather than a sampling error), then the remaining endbulbs (n=35) did not display size differences with respect to fiber CF or subdivisions within the AVCNa (Table 2). Endbulb size did not vary as a function of SR groupings (Fig. 13B), since those from high SR fibers were 215.9 ± 20.84 μm^2 compared to 216.35 ± 30.45 μm^2 for those from low and medium SR fibers.

DISCUSSION

The present study in mature cats analyzed the morphology of endings arising from the axons of type I spiral ganglion neurons and terminating in the cochlear nucleus. The endings ranged widely in size, shape, and complexity from the simple terminal bouton to the large endbulb of Held. Due to this diversity, separate categories were defined on the basis of ending shape; there were simple endings, string endings, and small, medium, and large complex endings. It

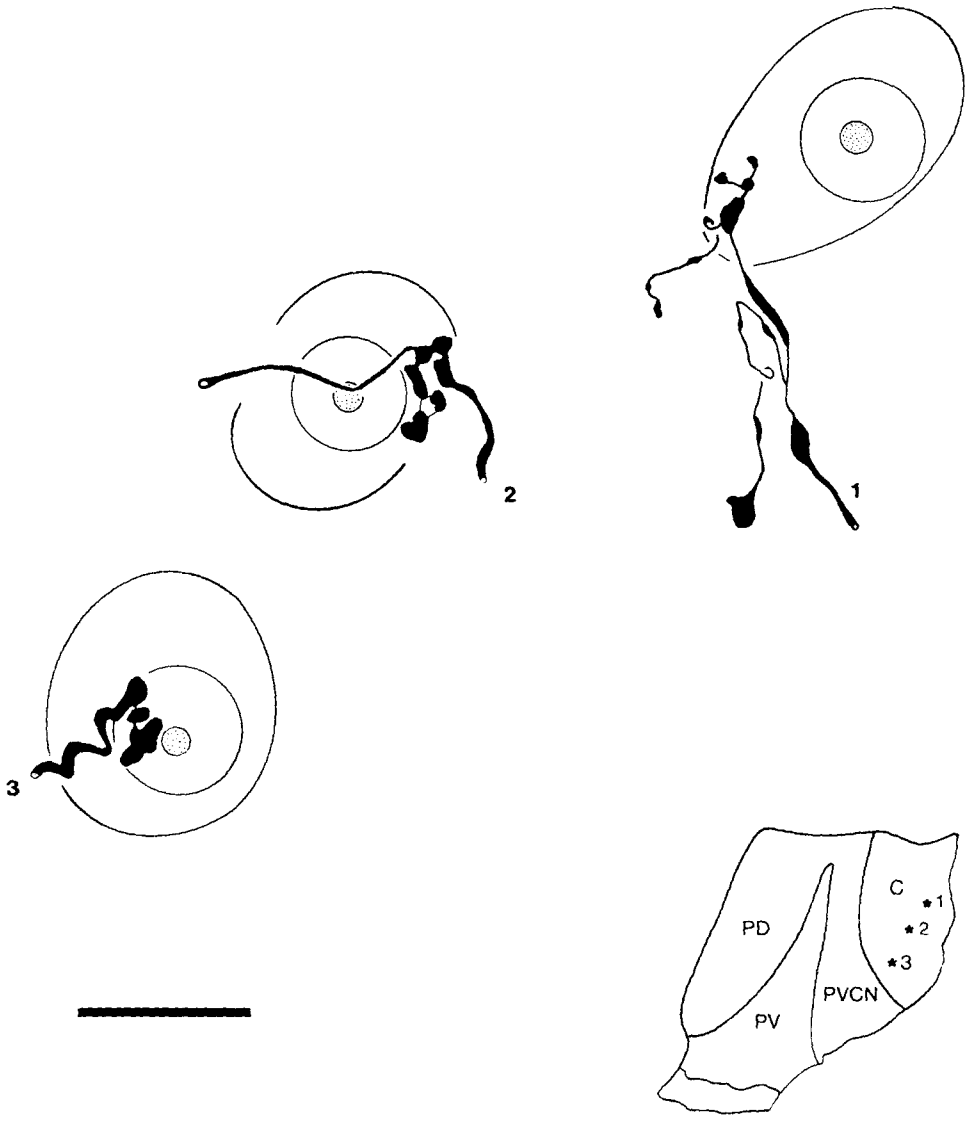

Fig. 10. Drawing tube reconstruction of medium-sized complex endings (modified endbulbs) in the central region of the PVCN. These endings arise from the DB and contact the cell bodies of octopus cells. Inset: location of endings (1, 2, 3). Abbreviations: C, central region of PVCN; PD, dorsal part of the AVCNp; PV, ventral part of the AVCNp. Scale bar equals 20 μm.

should be stressed that size is represented by area measurements calculated from the silhouettes of endings projected onto a plane. This measure appears sufficient for estimating the "sizes" of simple ellipsoidal or spherical structures, such as most terminal boutons or the individual elements of string endings. The method may be less appropriate for estimating sizes of more complex structures, such as endbulbs of Held. For example, orientation and size can determine the extent to which one part of a complicated ending overlaps with another part. By our method of estimating sizes, the greater the overlap, the greater the difference between silhouette area and "actual" area. Since there was no evidence for systematic variations in orientation of the complicated endings, our measurements underestimate area for some of the larger structures but do not alter relative size relationships among the different ending categories. At present, certain "trends" are revealed with respect to structure-function relationships, but the sample size (number of cats and number of fibers) is still sufficiently small that caution is advised when interpreting the results.

Relation to Golgi descriptions in kittens

For the most part, the endings in cats are simply more "mature" versions of those described in the classical kitten material prepared by Golgi techniques (Held, 1893; Vincenzi, '01; Ramón y Cajal, '09; Brawer and Morest, '75; Lorente de Nó, '81). Maturational changes in endbulb morphology (Ryugo and Fekete, '82) and primary collateral arborizations (Schweitzer and Cant, '84; Fekete et al., '84) have been previously discussed. There are, however, other age-related issues that merit further comment. For example, it has previously been reported in kittens and other small mammals that the size of endbulbs from the ascending branch is greatest rostrally and diminishes progressively in more posterior regions as the auditory nerve root is approached (Ramón y Cajal, '09; Lorente de Nó, '79). We

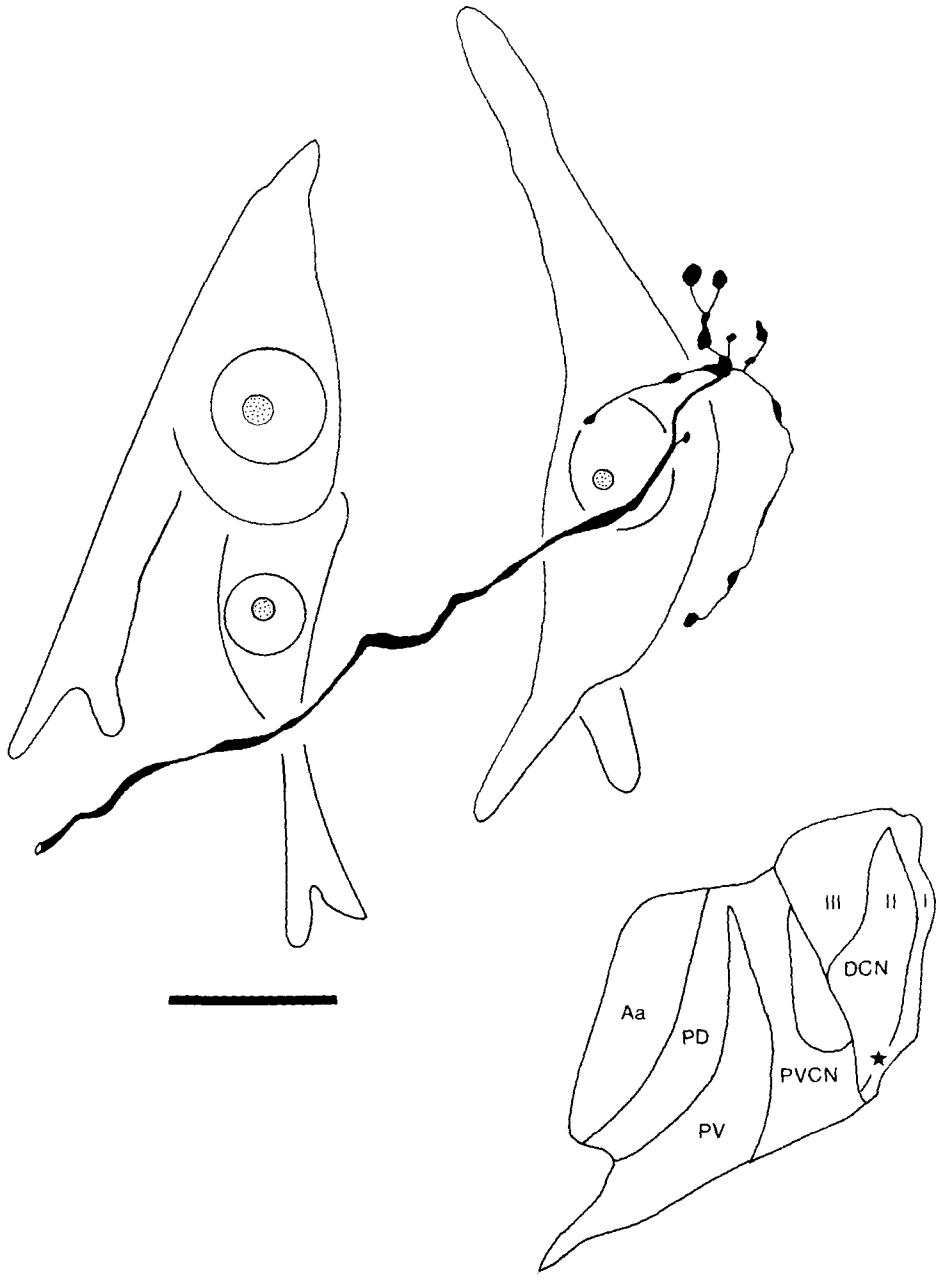

Fig. 11. Drawing tube reconstruction of medium-sized complex ending in the DCN. This ending terminates primarily in the neuropil of layer II but does send a bouton and *en passant* swelling to contact the cell body of a pyramidal cell. These larger endings were not commonly observed along the DB. Inset: location of ending is indicated by the star. Abbreviations: Aa, anterior division of the AVCN; I, layer I or molecular layer of DCN; II, layer II or pyramidal cell layer of DCN; III, layer III or deep polymorphic layer. Scale bar equals 20 μm.

found many exceptions to this generalization as indicated by the considerable variation in endbulb size both within and across subdivisions of the AVCNa. By using larger regions, however, a rough gradient for endbulb size could be observed according to relative anterior-posterior position within the nucleus (Tables 1,2). This observation is in agreement with the relative size relationship described in neonatal kitten material (Brawer and Morest, '75). Based on the relatively constant distribution of endbulbs with respect to size and subdivision at different ages, it seems that the large and small spoonlike endings in kittens, respectively, mature into the large and small complex (reticulated) endings in cats.

With respect to the DB, we did not observe what has been referred to as "pericellular baskets" generated by single fibers in the PVCN of kittens (e.g., as illustrated in Figs. 330, 332: Ramón y Cajal, '09). Extracellular injections of HRP into the auditory nerve of mature cats label many fibers whose overall pattern in the PVCN produces pericellular baskets (unpublished observations). These different innervation patterns of the PVCN for cats at different ages suggest that single fibers in immature animals have greater branching and more extensive arbors (necessary to form a pericellular basket) than in mature animals (where several fibers are required to form a single plexus). Such a conclusion, however, conflicts with other observations suggesting

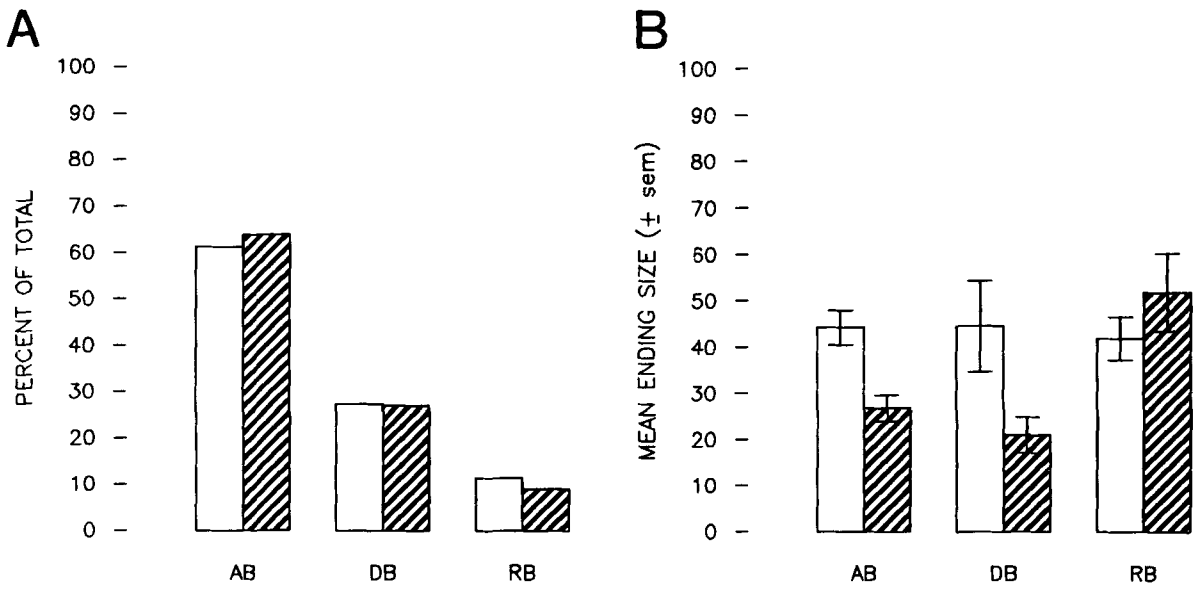

Fig. 12. A. Bar graph illustrating relative branch distribution for all medium complex endings from fibers of high SR (n=44, open bars) and low and medium SR (n=33, striped bars). The relative distribution does not change with respect to fiber SR. B. Bar graph illustrating that medium complex endings from low and medium SR fibers (striped bars) are not significantly smaller than those from high SR fibers (open bars) when analyzed according to parent branch of origin: AB, p=n.s.; DB, p=n.s. Root branch measurements may not be reliable because of the small sample size.

TABLE 1. Endbulbs: Sizes and Regional Distribution in the AVCN

Region	n	Mean size	SEM	CF range (kHz)
Terminal endbulbs (n = 27)				
AA	18	246.2	27.76	0.3–12.0
APD	3	173.0	33.01	25.0–36.0
AA/AP	3	343.0	44.16	0.3–0.6
AP	3	246.1	68.79	2.7–4.0
PD	0	—	—	—
PV	0	—	—	—
Collateral endbulbs (n = 18)				
AA	1	142.1	—	
APD	0	—	—	
AA/AP	1	483.1	—	
AP	2	205.3	11.56	
PD	7	164.2	33.51	
PV	7	116.9	18.26	
All endbulbs (n = 45)				
AA	19	240.7	26.81	
APD	3	173.0	33.01	
AA/AP	4	378.0	44.90	
AP	5	229.8	42.32	
PD	7	164.6	33.51	
PV	7	116.9	18.26	

[1]AA, anterior part; APD, posterodorsal part; AP, posterior part; PD and PV, dorsal and ventral parts of the posterior division of the AVCN.

TABLE 2. Regional Analysis of Endbulb Size[1]

Region	n	Mean size	SEM
Large endbulbs[2]			
AA	5	403.9	8.76
APD	0	—	—
AA/AP	3	424.8	25.78
AP	1	409.1	—
PD	1	310.9	—
PV	0	—	—
Small endbulbs[3]			
AA	14	182.4	15.88
APD	3	173.0	33.01
AA/AP	1	237.6	—
AP	4	184.9	17.30
PD	6	140.2	28.98
PV	7	116.9	18.26

[1]Abbreviations as in Table 1. CF, characteristic frequency.
[2]n = 10, area > 300 μm^2, CF < 4 kHz.
[3]n = 35, area < 300 μm^2, CF = 0.3 – 36 kHz.

that arbors of auditory nerve fibers elaborate during postnatal maturation (Schweitzer and Cant, '84; Fekete et al., '84). Alternatively, it may be that some of the early Golgi work did not always describe details at the single cell level, especially since the tracing of collaterals back to individual auditory nerve fibers was not explicitly stated.

In the central region of PVCN (octopus cell region), neurons having cytological features of octopus cells (criteria of Osen, '69) were associated with one of two patterns of primary endings. They would receive relatively small endings (terminal boutons, string endings, or small complex endings) on their dendrites or perikarya by way of "collateral cascades" (see Fekete et al., '84) or they would receive a modified endbulb on their cell body. In our limited sample, a single fiber did not give rise to both kinds of endings onto the same cell. These distinct patterns of primary input suggest that octopus cells as defined by Nissl criteria may actually represent additional subtypes. Such a notion is consistent with electrophysiological data revealing more than one unit type in this region (Godfrey et al., '75a; Ritz and Brownell, '82). We were particularly interested in the collaterals of the central region because of Kane's ('73) report of heterotypic synapses onto octopus cells. We were unable to verify her basic observation that two distinct classes of endings (large and small boutons) arise from a single fiber and converge onto the same octopus cell. In our material, large and small ending types remained segregated, and bouton size was neither as uniform nor as closely correlated with preterminal collateral diameter as described by Kane ('73). These descriptive differences may be due to maturational changes in axon arbors or bouton appearance.

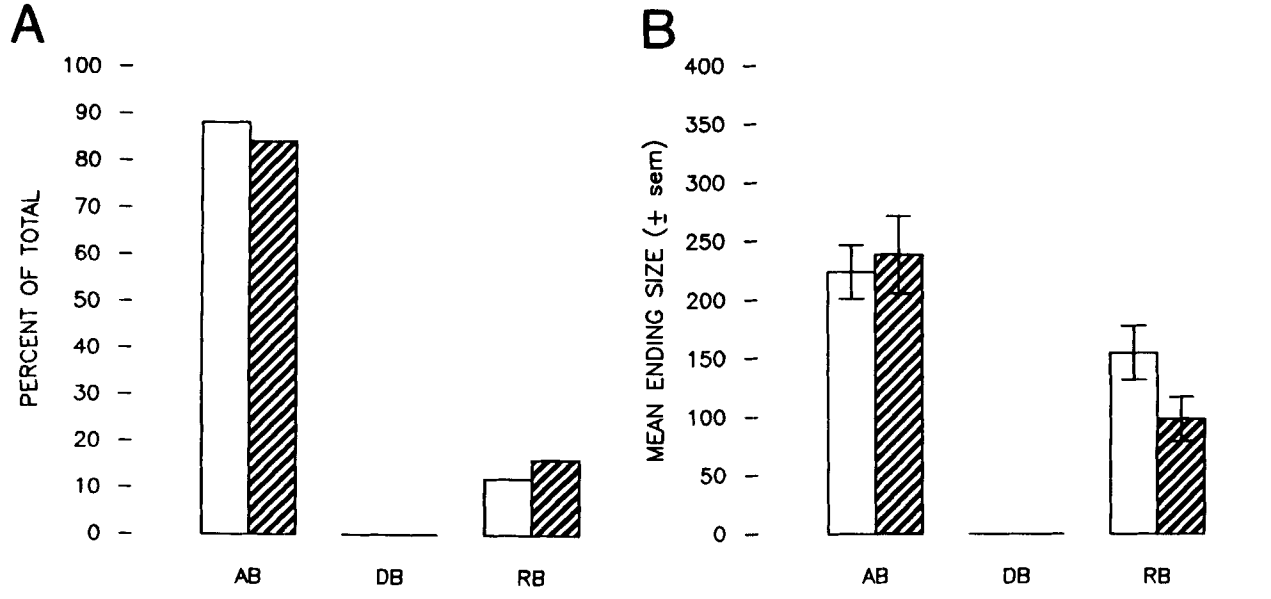

Fig. 13. A. Bar graph illustrating relative branch distribution for all large complex endings from fibers of high SR (n=26, open bars) and low and medium SR (n=19, striped bars). The relative distribution does not vary according to fiber SR. B. Bar graph illustrating that large complex endings from low and medium SR fibers (striped bars) are generally the same size as those from high SR fibers (open bars): AB, P=n.s.; DB, no endings. Root branch measurements may not be reliable because of the small sample size.

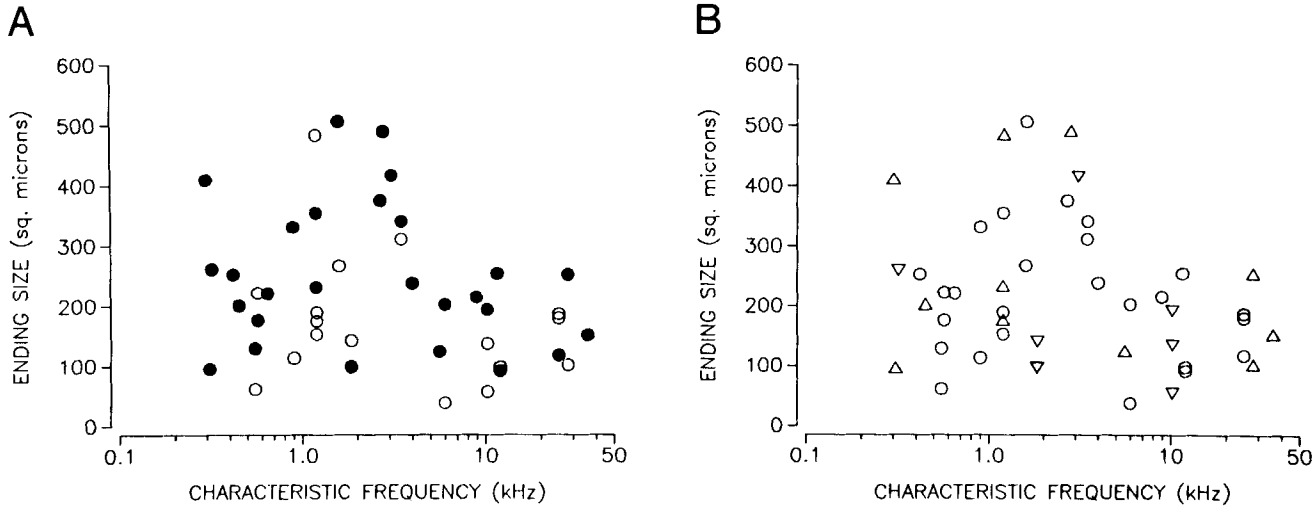

Fig. 14. Scatter plots illustrating the distribution of endbulb size with respect to fiber CF. A. Comparison between terminal endbulbs (filled circles) and collateral endbulbs (open circles). Note that largest endbulbs arise from fibers having CFs below 4 kHz. B. Comparison between endbulbs from fibers of low (▽), medium (△), and high (○) SR groups.

The presence of modified endbulbs in the region of the auditory nerve root has been described for kittens (Ramón y Cajal, '09; Lorente de Nó, '81), cats (Fekete et al., '84), and rats (Harrison and Irving, '66). We observed modified endbulbs distinctly outside the region of the nerve root, in the multipolar cell region and central region of the PVCN. These infrequent endings appeared like those found in the AVCN and made axosomatic contact with globular and octopus cells. Such endings in the PVCN may be related to the "unusually large boutons" defined by Lorente de Nó (and illustrated in Figs. 4–8: '81).

In rare cases, we observed relatively large endings in the DCN. There is one ending in the present data base that forms a prominent "spray" of collaterals, but this spray terminates primarily in the neuropil. These endings presumably correspond to the "gigantic endings" of the kitten DCN that were defined by Lorente de Nó (and illustrated in Fig. 6-6: '81). It is possible that the medium-sized axosomatic endings of the PVCN and DCN in adult cats develop from clublike structures resembling growth cones in kittens, in a manner analogous to the postnatal maturation of endbulbs of Held in the AVCN (Ryugo and Fekete, '82).

Ending categories

Terminal boutons are the most common ending type, and the endbulbs of Held are the most conspicuous. Held (1893)

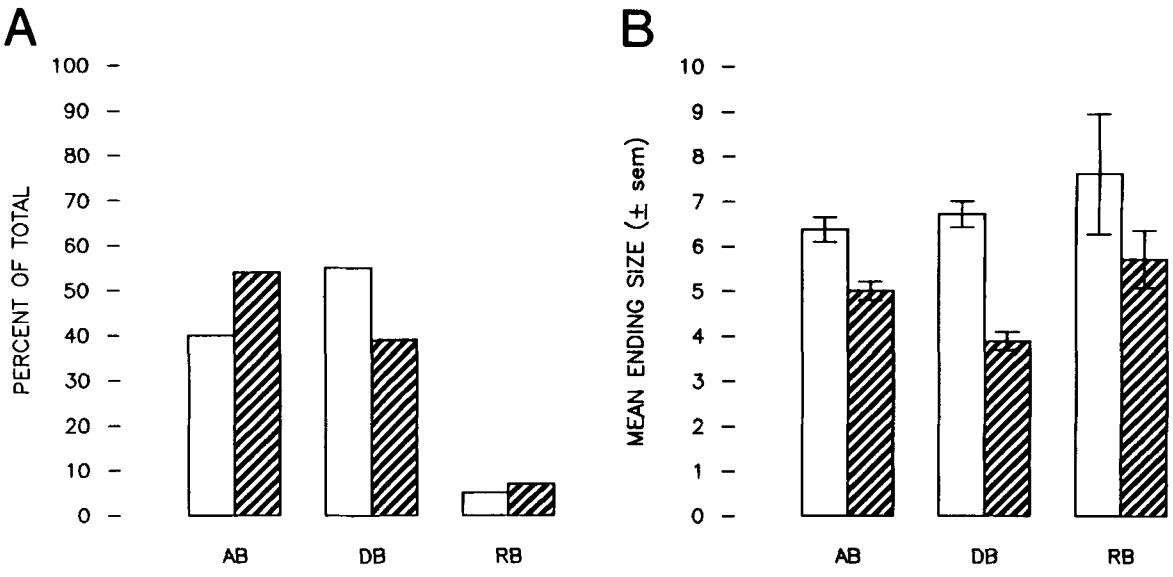

Fig. 15. A. Bar graph illustrating relative branch distribution for the combined category of small endings (simple endings, string endings, and small complex endings) from fibers of high SR (n=807, open bars) and low and medium SR (n=1,131, striped bars). The relative distribution does vary according to fiber SR. B. Bar graph illustrating that small endings from low and medium SR fibers (striped bars) are smaller than those from high SR fibers (open bars): AB, $P < .001$; DB, $P < .001$; RB, P=n.s.

originally suggested that boutons and endbulbs were the two types of endings emitted from auditory nerve fibers based on analysis of kitten Golgi material, a conclusion generally supported by subsequent investigations in other mammals (e.g., Ramón y Cajal, '09; Lorente de Nó, '33; Harrison and Irving, '66; Brawer and Morest, '75). In the mature cat, the majority of endings fall into one of these two groups, although some endings have distinctly intermediate characteristics. The group of small endings consists of simple endings, string endings, and small complex endings. They have been grouped together because they share a relatively simple shape, they are small in size, and they have features that vary predictably with respect to fiber SR (Fig. 15). The group of intermediate endings consists of modified endbulbs, and the group of large endings consists of the endbulbs of Held.

All ending types were found on the AB and all but endbulbs were found on the DB. As a result, there is a considerable range in ending sizes within the VCN. In contrast, the DCN contains a more homogeneous population of primary endings, characterized mostly by simple endings and small complex endings. Despite the variation in morphological appearance, HRP-labeled endings in adult cats could be placed into one of three descriptive categories on the basis of size and shape. Furthermore, each category showed specific characteristics with respect to spatial distribution in the cochlear nucleus.

Morphological correlates of CF

The present data revealed a CF-related specialization of ending morphology that was confined exclusively to the category composed by endbulbs of Held. The largest endbulbs arose from fibers having relatively low CFs (below 4 kHz) whereas smaller endbulbs arose from fibers of all CFs. Since terminal endbulb size is highly correlated with postsynaptic (spherical) cell body size but not CF (Fekete, '84), a strict size gradient of spherical cells associated with CF should not be expected. Instead, the largest spherical cells should be distributed below the 4-kHz isofrequency contour. The functional significance of this morphological discontinuity at 4 kHz is presently unknown, but the basic observation may be relevant to other phenomena. For instance, all of the spiral ganglion neurons in the top 20th percentile according to cell body size (silhouette area) have CFs below 4 kHz (Liberman and Oliver, '84). Perhaps neurons with large cell bodies simply give rise to large endbulbs.

On the other hand, 4 kHz approximates the upper frequency limit for unambiguous binaural phase cues for the cat (Casseday and Neff, '73) and where auditory nerve fibers no longer transmit impulses "locked" to the phase of the stimulus (Kiang et al., '65; Rose et al., '67). Below this frequency limit, the response of many cochlear nucleus neurons is also locked to the phase of sinusoidal stimuli, especially in the AVCN (e.g., Lavine, '71; Rose et al., '74; Bourk, '76). This reliable temporal relationship of neural discharge to a particular phase of sinusoid stimuli is thought to provide a basis for processing binaural time differences at more central levels of the auditory system. For example, binaural neurons in the medial superior olive exhibit responses which are dependent on the coincidence of phase-locked discharges emanating from the cochlear nuclei on both sides of the brain (Goldberg and Brown, '68). The faithful preservation of such timing information requires high-fidelity transmission through the cochlear nucleus. If size of an ending is related to synaptic efficiency, then neurons of the AVCN that exhibit the highest degree of phase-locking may be the same ones that receive the very largest endbulbs.

There is numerical and spatial correspondence of cell type, ending type, and unit type in the AVCN (e.g., Brawer et al., '74; Bourk, '76). Such observations have prompted the notion that synaptic drive provided by endbulbs accounts for the preservation by cochlear nucleus cells of the "primarylike" discharge patterns conveyed by auditory nerve fibers (Kiang, '75). Endbulbs contact spherical cells in the AVCNa and less frequently contact globular cells in

the AVCNp. The smaller modified endbulbs should have correspondingly smaller postsynaptic effects, and they contact globular cells in the AVCNp and an occasional spherical cell in the AVCNa. It is hypothesized that several modified endbulbs must converge onto the same cell (globular or spherical) and discharge in unison to produce a postsynaptic action potential. The synchronous presynaptic activity that results in a postsynaptic discharge and refractory period is thought to be responsible for creating the "notch" in the primarylike-with-notch discharge pattern (Bourk, '76). Since morphologically different cell types in the cochlear nucleus (based on dendritic or Nissl criteria) can receive similar types of primary input, they should also exhibit similar response patterns. Likewise, morphologically similar cell types can receive different kinds of primary input and exhibit different response patterns. Such a conclusion represents a modification of structure-function relationships formulated from previous correlations but is consistent with more recent observations derived from intracellular marking studies in this nucleus (Rouiller and Ryugo, '84).

On the basis of endbulb input, spherical cells should have CFs over the same range as auditory nerve fibers. A similar conclusion was reached on the basis of extracellular single unit recordings in the AVCN (Bourk et al., '81). In contrast, Osen ('70) had suggested that the rostrally located large spherical cell region should contain only low-to-middle CF neurons on the basis of comparing the course and termination of degenerating primary afferents. The region immediately caudal to the rostral pole was said to contain primarily small spherical cells. This small spherical cell region was presumed to represent the entire frequency range since it was intercepted by primary fibers originating from all segments of the organ of Corti. These specializations were further hypothesized to be related to specializations in the superior olivary complex (Osen, '70). The large spherical cell region was proposed to innervate the medial superior olive (MSO), which contained mostly units of low CFs; the small spherical cell region was proposed to innervate the lateral superior olive (LSO), which contained units spanning the CF range. It now appears, however, that the largest spherical cells should be located ventral to the 4-kHz isofrequency plane and smaller spherical cells should be distributed throughout the AVCNa. Furthermore, spherical cells of various sizes throughout the AVCNa project to both the lateral and medial superior olivary nuclei (Cant and Morest, '84). It is unknown whether an individual spherical cell projects to both targets, and it remains to be determined how the different frequency representation of the LSO and MSO (Guinan et al., '72; Tsuchitani, '77) might be related to the specializations of spherical cells. The possibility that auditory pathways may be separated according to frequency range is at least consistent with the notion that different cues are used to localize high- and low-frequency tones (e.g., Masterton et al., '75).

Morphological correlates of SR

Current data for single fiber recordings in the auditory nerve reveal that neurons having very different SRs can be found at all CF regions. Systematic differences in response properties under a wide variety of stimulus conditions characterize units belonging to separate SR groups and imply that these different SR unit types play fundamentally different roles in acoustic information processing (Liberman, '78; Sachs and Young, '79; Evans and Palmer, '80; Costalupes, '85). Differences in SR have been shown to correlate with differences in the caliber of the peripheral terminal and the location of the peripheral synapse on the inner hair cell (Liberman, '82s). Centrally, low and medium SR fibers have more highly branched and more widely distributed axonal arbors than those of high SR fibers, a feature that is confined to the ascending branch (Fekete et al., '84). One implication is that low and medium SR fibers have a wide distribution of many small postsynaptic effects throughout the AVCN.

The sizes of endings from low and medium SR fibers were distinctly smaller than those from high SR fibers. Endbulbs were an exception, but the present method of representing "size" by ending silhouette area might be admittedly insensitive to modest changes in such relatively large structures. Nevertheless, these SR-related size differences among endings appeared similar (at least in concept) to the activity-dependent shape changes reported in other neural and secretory systems (Heuser and Reese, '73; Pysh and Wiley, '74; Boyne et al., '75; Burwen and Satir, '77; Boyne and McLeod, '79). It is tempting to speculate that these SR-related size differences in terminal endings are due to the coalescence of synaptic vesicle membrane with the plasma membrane. Furthermore, these larger endings of high SR fibers might be preferentially accompanied by subcellular structures (e.g., coated vesicles) implicated in membrane retrieval and recycling.

In addition, there is circumstantial evidence that suggests that low and medium SR fibers may be part of a neural circuit involved with middle ear muscle reflex. The middle ear muscle reflex occurs in the presence of a loud noise whereby muscles of the middle ear contract and exert feedback control on the cochlear response (Borg, '72). The sensory limb of this acoustic reflex passes through the auditory nerve. Because the unmyelinated fibers of type II spiral ganglion cells have too long a conduction time (greater than 10 msec) to permit their participation in the earliest stages of the reflex (Kiang et al., '83), the myelinated axons of type I spiral ganglion cells must represent the important afferent source. Of the type I units, low and medium SR units have relatively high thresholds and therefore are still within their operating range in the presence of loud sounds. At high stimulus levels, low and medium SR units exhibit a striking increase in discharge rate over that seen at moderate stimulus levels whereas the response of high SR units remains saturated at both levels (Liberman and Kiang, '84). This response feature of low and medium SR fibers to loud sounds occurs at stimulus levels that coincide with the threshold of the middle ear muscle reflex. Acoustic reflex neurons apparently reside in the AVCN since there is no change in the reflex following transection of the major output pathways for the DCN and PVCN (the dorsal and intermediate acoustic striae, respectively), and transection of the output pathway for AVCN abolishes the reflex (Borg, '73). Recall that it is in the AVCN where the ABs of low and medium SR fibers are highly ramified. It is possible that low and medium SR fibers could be responsible for selectively activating a high-threshold circuit whose output is delivered to motoneurons of the middle ear muscles. The reflex circuit could include a distinct morphological class of neurons having widespread distribution throughout the AVCN (such as small cells or multipolar cells), or a heterogeneous confederacy of neurons whose common bond is contributing to the reflex. At present, however, there are no compelling neuronal candidates in the AVCN for proposing either kind of circuit.

ACKNOWLEDGMENTS

The authors gratefully acknowledge the technical contributions made by T.R. Bourk, M. Curby, L. Dodds, P. Ley, P. McGaffigan, B. Norris, M. Oliver, and D. Steffens, and the typing assistance provided by S. McDevitt and R.G. Vega. Some of the labeled fibers came from a previous collaborative effort with Dr. M. Charles Liberman. We thank Drs. T.E. Benson, N.Y.S. Kiang, and J.B. Kobler for helpful discussions of the data. This work was supported by NIH grants P01 NS13126 and R01 NS20156 and by the William F. Milton Fund of Harvard Medical School. E.M.R. was supported by the Swiss Foundation for Fellowships in Medicine and Biology (Basel, Switzerland). D.M.F. was supported in part by an NSF predoctoral fellowship and by a Ryan Foundation fellowship (Cincinnati, Ohio). Portions of these results were presented in preliminary form at the thirteenth meeting of the Society for Neuroscience, Boston, MA, 1983.

LITERATURE CITED

Borg, E. (1972) Acoustic middle ear reflexes: A sensory control system. Acta Otolaryngol. [Suppl.] *304*:1–34.

Borg, E. (1973) On the neuronal organization of the acoustic middle ear reflex. A physiological and anatomical study. Brain Res. *49*:101–123.

Bourk, T.R. (1976) Electrical Responses of Neural Units in the Anteroventral Cochlear Nucleus of the Cat. Cambridge, MA: Massachusetts Institute of Technology, Ph.D. Dissertation.

Bourk, T.R., J.P. Mielcarz, and B.E. Norris (1981) Tonotopic organization of the anteroventral cochlear nucleus of the cat. Hearing Res. *4*:215–241.

Boyne, A.F., and S. McLeod (1979) Ultrastructural plasticity in stimulated nerve terminals: Pseudopodial invasions of abutted terminals in *torpedine* ray electric organ. Neuroscience *4*:615–624.

Boyne, A.F., T.P. Bohan, and T.H. Williams (1975) Changes in cholinergic synaptic vesicle populations and the ultrastructure of the nerve terminal membranes of *narcine brasiliensis* electric organ stimulated to fatigue *in vivo*. J. Cell Biol. *67*:814–825.

Brawer, J.R., and D.K. Morest (1975) Relations between auditory nerve endings and cell types in the cat's anteroventral cochlear nucleus seen with the Golgi method and Nomarski optics. J. Comp. Neurol. *160*:491–506.

Brawer, J.R., D.K. Morest, and E.C. Kane (1974) The neuronal architecture of the cochlear nucleus of the cat. J. Comp. Neurol. *155*:251–300.

Burwen, S.J., and B.H. Satir (1977) Plasma membrane folds on the mast cell surface and their relationship to secretory activity. J. Cell Biol. *74*:690–697.

Cant, N.B., and D.K. Morest (1979a) Organization of the neurons in the anterior division of the anteroventral cochlear nucleus of the cat. Light microscopic observations. Neuroscience *4*:1909–1923.

Cant, N.B., and D.K. Morest (1979b) The bushy cells in the anteroventral cochlear nucleus of the cat. A study with the electron microscope. Neuroscience *4*:1925–1945.

Cant, N.B., and D.K. Morest (1984) The structural basis for stimulus coding in the cochlear nucleus of the cat. In: C.I. Berlin (ed.): Hearing Science: Recent Advances. San Diego: College-Hill Press, pp. 371–421.

Casseday, J.H., and W.D. Neff (1973) Auditory localization: Role of auditory pathways in brain stem of the cat. J. Neurophysiol. *36*:842–858.

Costalupes, J.A. (1985) Representation of tones in noise in the responses of auditory nerve fibers in cats. I. Comparisons with detection thresholds. J. Neurosci. *5*:3261–3269.

Evans, E.F., and A.R. Palmer (1980) Relationship between the dynamic range of cochlear nerve fibers and their spontaneous activity. Exp. Brain Res. *40*:115–118.

Fekete, D.M. (1984) Central Projections of Auditory Nerve Fibers in Cats. Cambridge, MA: Harvard University, Ph.D. Dissertation.

Fekete, D.M. E.M. Rouiller, M.C. Liberman, and D.K. Ryugo (1984) The central projections of intracellularly labeled auditory nerve fibers in cats. J. Comp. Neurol. *229*:432–450.

Feldman, M.L., and J.M Harrison (1969) The projection of the acoustic nerve to the ventral cochlear nucleus of the rat. A Golgi study. J. Comp. Neurol. *137*:267–294.

Godfrey, D.A., N.Y.-S. Kiang, and B.E. Norris (1975a) Single unit activity in the posteroventral cochlear nucleus of the cat. J. Comp. Neurol. *162*:247–268.

Godfrey, D.A. N.Y.-S. Kiang, and B.E. Norris (1975b) Single unit activity in the dorsal cochlear nucleus of the cat. J. Comp. Neurol. *162*:269–284.

Goldberg, J.M., and P.B. Brown (1968) Response of binaural neurons of dog superior olivary complex to dichotic tonal stimuli: Some physiological mechanisms of sound localization. J. Neurophysiol. *32*:613–636.

Guinan, J.J. Jr., B.E. Norris, and S.S. Guinan (1972) Single auditory units in the superior olivary complex. II: Locations of unit categories and tonotopic organization. Intern. J. Neurosci. *4*:147–166.

Harrison, J.M., and R. Irving (1966) The organization of posteroventral cochlear nucleus in the rat. J. Comp. Neurol. *126*:391–402.

Held, H. (1893) Die centrale Gehorleitung. Arch. Anat. Physiol. *17*:201–248.

Heuser, J.E., and T.S. Reese (1973) Evidence for recycling of synaptic vesicle membrane during transmitter release at the frog neuromuscular junction. J. Cell Biol. *57*:315–344.

Ibata, Y, and G.D. Pappas (1976) The fine structure of synapses in relation of the large spherical neurons in the anterior ventral cochlear (sic) of the cat. J. Neurocytol. *5*:395–406.

Kane, E.C. (1973) Octopus cells in the cochlear nucleus of the cat: Heterotypic synapses upon homeotypic neurons. Intern. J. Neurosci. *5*:251–279.

Kettner, R.E., J. Feng, and J.F. Brugge (1984) Postnatal development of the phase-locked response to low frequency tones of auditory nerve fibers in the cat. J. Neurosci. *5*:275–283.

Kiang, N.Y.-S. (1975) Stimulus representation in the discharge pattern of auditory neurons. In: D.B. Tower (ed.): The Nervous System, Vol. 3, Human Communication and its Disorders. New York: Raven Press, pp. 81–96.

Kiang, N.Y.-S., T. Watanabe, E.C. Thomas, and L.F. Clark (1965) Discharge Patterns of Single Fibers in the Cat's Auditory Nerve. Cambridge: MIT Press.

Kiang, N.Y.-S., E.M. Keithley, and M.C. Liberman (1983) The impact of auditory nerve experiments on cochlear implant design. Ann. N.Y. Acad. Sci. *405*:114–121.

Lavine, R.A. (1971) Phase-locking in response of single neurons in cochlear nuclear complex of the cat to low-frequency tonal stimuli. J. Neurophysiol. *34*:467–483.

Lenn, N.Y., and T.S. Reese (1966) The fine structure of nerve endings in the nucleus of the trapezoid body and the ventral cochlear nucleus. Am. J. Anat. *118*:375–389.

Liberman, M.C. (1978) Auditory-nerve response from cats raised in a low-noise chamber. J. Acoust. Soc. Am. *63*:442–455.

Liberman, M.C. (1982a) Single-neuron labelling in the cat auditory nerve. Science *216*:1239–1241.

Liberman, M.C. (1982b) The cochlear frequency map for the cat: Labelling auditory-nerve fibers of known characteristic frequency. J. Acoust. Soc. Am. *72*:1441–1449.

Liberman, M.C., and N.Y.-S. Kiang (1984) Single-neuron labeling and chronic cochlear pathology. IV. Stereocilia damage and alterations in rate- and phase-level functions. Hear. Res. *16*:75–90.

Liberman, M.C., and M.E. Oliver (1984) Morphometry of intracellularly labeled neurons of the auditory-nerve: Correlations with functional properties. J. Comp. Neurol. *223*:163–176.

Lorente de Nó, R. (1933) Anatomy of the eighth nerve. III. General plan of structure of the primary cochlear nuclei. Laryngoscope *43*:327–350.

Lorente de Nó, R (1979) Central representation of the eighth nerve. In: V. Goodhill (ed.): Ear: Diseases, Deafness and Dizziness. New York: Harper & Row Publishers, pp. 64–86.

Lorente de Nó, R. (1981) The Primary Acoustic Nuclei. New York: Raven Press.

Masterton, R.B., G.C. Thompson, J.K. Bechtold, and M.R. RoBards (1975) Neuroanatomical basis of binaural phase-difference analysis for sound localization: A comparative study. J. Comp. Physiol. Psychol. *89*:379–386.

Mugnaini, E., W.B. Warr, and K.K. Osen (1980) Distribution and light microscopic features of granule cells in the cochlear nucleus of cat, rat, and mouse. J. Comp. Neurol. *191*:581–606.

Osen, K.K. (1969) Cytoarchitecture of the cochlear nuclei in the cat. J. Comp. Neurol. *136*:453–484.

Osen, K.K. (1970) Course and termination of the primary afferents in the cochlear nuclei of the cat: An experimental anatomical study. Arch. Ital. Biol.*108*:21–51.

Pfeiffer, R.R. (1966) Classification of response patterns of spike discharges for units in the cochlear nucleus: Tone burst stimulation. Exp. Brain Res. *1*:220–235.

Pujol, R., E. Carlier, and C. Devigne (1978) Different patterns of cochlear innervation during the development of the kitten. J. Comp. Neurol. *177*:529–536.

Pujol, R., E. Carlier, and C. Devigne (1979) Significance of presynaptic formations in early stages of cochlear synaptogenesis. Neurosci. Lett. *15*:97–102.

Pysh, J.J., and R.G. Wiley (1974) Synaptic vesicle depletion and recovery in cat sympathetic ganglia electrically stimulated *in vivo*. Evidence for transmitter release by exocytosis. J. Cell Biol *60*:365–374.

Ramón y Cajal, S. (1909) Histologie du Système Nerveux de l'Homme et des Vertébrés, Vol. I. Instituto Ramón y Cajal (1952 reprint), Madrid, pp. 754–838.

Ritz, L.A., and W.E. Brownell (1982) Single unit analysis of the posteroventral cochlear nucleus of the decerebrate cat. Neuroscience 7:1995–2010.

Romand, R. (1984) Functional properties of auditory-nerve fibers during postnatal development in the kitten. Exp. Brain Res. *56*:395–402.

Romand, R., A. Sans, M.R. Romand, and R. Marty (1976) The structural maturation of the stato-acoustic nerve in the cat. J. Comp. Neurol. *170*:1–16.

Romand, R., M.R. Roman, Ch. Malle, and R. Marty (1980) Early stages of myelination in the spiral ganglion cells of the kitten during development. Acta Otolaryngol. *90*:391–397.

Rose, J.E., J.F. Brugge, D.J. Anderson, and J.E. Hind (1967) Phase-locked response to low-frequency tones in single auditory nerve fibers of the squirrel monkey. J. Neurophysiol. *30*:769–793.

Rose, J.E., L.M. Kitzes, M.M. Gibson, and J.E. Hind (1974) Observations on phase-sensitive neurons of anteroventral cochlear nucleus of the cat: Nonlinearity of cochlear output. J. Neurophysiol. *37*:218–253.

Rouiller, E.M., and D.K. Ryugo (1984) Intracellular marking of physiologically characterized neurons in the ventral cochlear nucleus of the cat. J. Comp. Neurol. *225*:167–186.

Ryugo, D.K., and D.M. Fekete (1982) Morphology of primary axosomatic endings in the anteroventral cochlear nucleus of the cat: A study of the endbulbs of Held. J. Comp. Neurol. *210*:239–257.

Sachs, M.B., and E.D. Young (1979) Encoding of steady-state vowels in the auditory nerve: Representation in terms of discharge rate. J. Acoust. Soc. Am. *66*:470–480.

Schweitzer, L., and N.B. Cant (1984) Development of the cochlear innervation of the dorsal cochlear nucleus of the hamster. J. Comp. Neurol. *225*:228–243.

Tolbert, L.P., and D.K. Morest (1982a) The neuronal architecture of the anteroventral cochlear nucleus of the cat in the region of the cochlear nerve root: Golgi and Nissl methods. Neuroscience 7:3013–3030.

Tolbert, L.P., and D.K. Morest (1982b) The neuronal architecture of the anteroventral cochlear nucleus of the cat in the region of the cochlear nerve root: Electron microscopy. Neuroscience 7:3053–3067.

Tsuchitani, C (1977) Functional organization of lateral cell groups of cat superior olivary complex. J. Neurophysiol. *40*:296–318.

Tsuchitani, C. (1978) Lower auditory brain stem structures of the cat. In R.F. Naunton and C. Fernandez (eds.): Evoked Electrical Activity in the Auditory Nervous System. New York: Academic Press, pp. 373–401.

Vincenzi, L. (1901) Sulla fina anatomia del nucleo ventrale dell'acustico. Anat. Anz. *19*:33–42.